Calculations of the Potential Energy Surface for a Water Molecule Dissociation on the Pt (111) Surface

Siti Zulaehah[1,2] Diska Nirmala Wahyu Dinasty[2] Allan Abraham Bustria Padama[3]
Wahyu Tri Cahyanto[2,*]

[1]*Department of Mechanical Engineering, Universitas Perwira Purbalingga, Jl. S. Parman, Purbalingga, 53313, Indonesia.*
[2]*Department of Physics, Universitas Jenderal Soedirman, Jl. Dr. Soeparno, Grendeng, Purwokerto, 53123, Indonesia.*
[3]*Materials Computations Group, Institute of Mathematical Sciences and Physics, University of the Philippines Los Baños, College, Los Baños, Laguna 4031, Philippines.*

[*]*Corresponding author. Email: wahyu.cahyanto@unsoed.ac.id*

ABSTRACT

We present a density functional theory (DFT) study of the dissociation pathway of monomeric H_2O into adsorbed hydroxyl (OH_{ads}) and hydrogen (H_{ads}) on the Pt(111) surface. Here we consider the Langmuir-Hinshelwood process of adsorbed monomeric H_2O, which is then dissociated on the surface model. By calculating potential energy surfaces (PESs), we examine the proposed pathways to determine the most likely ones. The results show that the activation energies of two reaction pathways are comparable within the experimental and theoretical results. This study should provide information to understand the mechanism of H_2O dissociation on the Pt(111) surface.

Keywords: *H_2O dissociation, reaction pathways, DFT, activation energy.*

1. INTRODUCTION

The water (H_2O) dissociative adsorption on metallic platinum (Pt) surfaces have found in lots of applications e.g. electrochemistry, heterogeneous catalyst, hydrogen production, and fuel cell devices [1–3]. Among the different route reaction of the water and metal surfaces, the net reaction process is the separation water into H_2 and O_2 as useful gases through the electro-oxidation process [4, 5]. To achieve this, the metallic platinum (Pt) based catalyst has showed high stability and activity that influencing the behaviour of the active surface toward the dissociation of water molecules [6–8]. There have so many experimental and theoretical studies about the water interaction on metal surfaces [9, 10]. On the surface, water forms different structure from monomer to ordered over-layers structures depending on the coverage and experimental conditions [11]. At the low coverages, the monomer water structure was observed by experiment which is less than 0.005 ML [12] and is stable as a monomer at temperatures of 40 K or less on transition metals [13]. To reveal the basic principles of the interaction of monomer H_2O with Pt catalyst, numerous studies have been undertaken in which the H_2O dissociative adsorption which generally believed to be rate determining steps [14–16]. Even though the dissociation of H_2O on Pt(111) surface to produce an oxidant (OH_{ads}) is very difficult [17], many efforts to developing and understanding the processes are still remain to be solved. The experimental and theoretical studies suggest the intermediate reaction process of H_2O dissociation to be OH_{ads} and H_{ads} on Pt based catalyst [18, 19]. As the mechanism of the dissociative adsorption of H_2O into OH_{ads} and H_{ads} on Pt(111) have been already explored, the dissociation energy barrier of $H_2O_{ads} \Rightarrow OH_{ads} + H_{ads}$ are in range of 0.75 eV − 1.80 eV [20] which might be inconsistent with the experimental results (0.52 eV) [21]. The detailed reasons for the disagreements and the complete dissociation processes have not been clarified yet. Moreover, the barriers will depends on the path of the reaction as well as the orientation of the adsorbed H_2O on Pt(111). Here, we extend the insight of dissociation

Copyright © 2022 The Authors. Published by Atlantis Press International B.V.
This is an open access article distributed under the CC BY-NC 4.0 license -http://creativecommons.org/licenses/by-nc/4.0/.

mechanism of H_2O into OH_{ads} and H_{ads} on Pt(111) by analysing the potential energy surfaces (PESs) scans from the ground state total energy calculation of density functional theory method. The starting point here will be an in-depth understanding the reaction path of monomer H_2O dissociation into OH_{ads} and H_{ads} by presenting the relatable energies pathways of H_2O dissociation on Pt(111) surface.

2. COMPUTATIONAL DETAILS

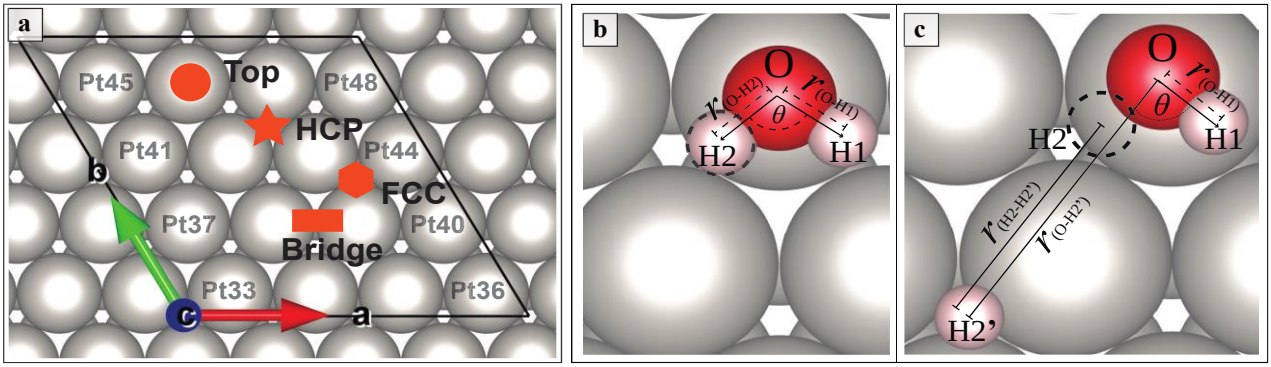

Figure 1: Schematic configurations of (a) the Pt(111) surface and the related adsorption sites ,i.e. top sites, hollow HCP site, hollow FCC sites and bridge sites. The (4 × 4) conventional unit cell is indicated by lattice vectors *a* and *b*. (b) The adsorption of monomer H_2O_{ads}/Pt(111) for initial state (IS) configuration, and (c) the co-adsorption of (OH_{ads}+H_{ads})/Pt(111) for final state (FS) configuration in determining the possible reaction pathways from PESs.

The density functional theory (DFT) formalism [22, 23] was used to calculate the total ground state energy interaction of monomeric H_2O molecule and Pt(111) carried out by vienna ab initio simulation package (VASP) [24, 25]. To describe the electron-ionic core interaction, the projector augmented wave (PAW) [26, 27] exchange-correlation functional with PW91 generalized gradient approximation [28–30] were used in this calculations. The electronic wave functions were expanded with cut-off energy of 400 eV as a plane wave basis. To perform the Brillouin zone integrations with (5×5 ×1) *k*-point mesh, we take up the Monkhorst and Pack method [31] with σ = 0.2 eV of Methfessel-Paxton smearing [32]. In reaching the convergence criteria, the maximum force acting on each atom were set to below 0.01 eV/Å, and 10^{-4} eV for the electronic self-consistent iteration for each atom. We use our previous configurations model of Pt(111) [33] by cleaving the crystal structure of (fcc) Pt with the bulk lattice parameter of 3.92 Å obtained from experiment [34]. We use four atomic layers, (4×4)-surface unit cell (Θ= 1/16ML) and a ~15Å of vacuum to avoid interaction between the surfaces of neighbouring slabs as described in figure 1(a). To simulate the adsorption of a H_2O and co-adsorption of OH_{ads} +H_{ads} on the Pt(111), we use our previous results from Ref. [35, 36] for initial state [IS] and final state [FS] configurations as presented in figure 1(b) and 1(c) respectively. Based on figure 1, we describe the dissociation pathways using potential energy surfaces (PESs) scan by separating the H2 atom into H2' position varies in terms of the shortest possible path on Pt (111) while OH1 being attached on top site of Pt43. In this study, we will concern only two pathways to obtain the energy barrier of H_2O_{ads} decomposition into OH_{ads} and H_{ads}. The transition states (TSs) is then defined as the state corresponding to the highest potential energy along this reaction coordinate of the PESs profile. Henceforth, the energy barrier (E*a*) for each path are calculated by the related potential energy difference of [H2'−OH1] distance on Pt(111) at TS and IS. Finally, the path with the most minimal energy is defined as the most possible pathway in dissociating H_2O into OH_{ads} and H_{ads}.

3. RESULTS AND DISCUSSION

To scan the PESs of the corresponding energy profile of H_2O dissociation, the IS and FS configuration of adsorbed H_2O /Pt(111) is crucial to determine the activation energy barrier (E*a*). In our previous results from Ref. [35, 36], the H_2O adsorb aligned parallel with Pt(111) and the distance of O−Pt [r_e(O−Pt)]=2.31 Å, the ∠(H1−O−H2) angle broadening to 105.7° and the adsorption energy was about −0.30 eV. This results are near to the results from Fajin *et al*. [37]. We then use this result (presented in figure 1(b)) as the IS configuration. The co-adsorption of (OH_{ads}+H_{ads})/Pt(111) configuration was also obtained from cf., e.g., [35, 36] and references therein as a (FS) configuration. The separated H2' at hollow fcc site position from OH1 is far enough to ensure that H2' already broken from its water configuration (presented in figure 1(c)). The distance of Pt−OH1 is *z*-(Pt−OH1) = 1.98 Å lower than its IS, and the *z*-(H2′ −Pt) = 0.77 Å. This configurations shows that the co-adsorption of (OH_{ads}+H_{ads})/Pt(111) is possible structure as the co-adsorption energy is negative (i.e., −0.63 eV). Based on the adsorption energy of H_2O/Pt(111) with this

physisorption energy, it can be assumed that the dissociation will proceed with difficult process as predicted by Hammer and Nørskov [38]. To predict the reaction mechanism of H_2O dissociation then we need to analyze the reaction path and geometry orientation. Here, we will focus on H_2O dissociation on Pt(111) for two reaction pathways by analyzing the PESs scan energies. The calculated results of the minimum energy of the H2' position (r, z) for each path are presented in figure 2 for reaction path number-1 and path number-2 respectively. In this case, the TSs of each path are obtained by the saddle point of PESs with respect to the H_2O adsorbed on Pt(111) surface along the reaction coordinates.

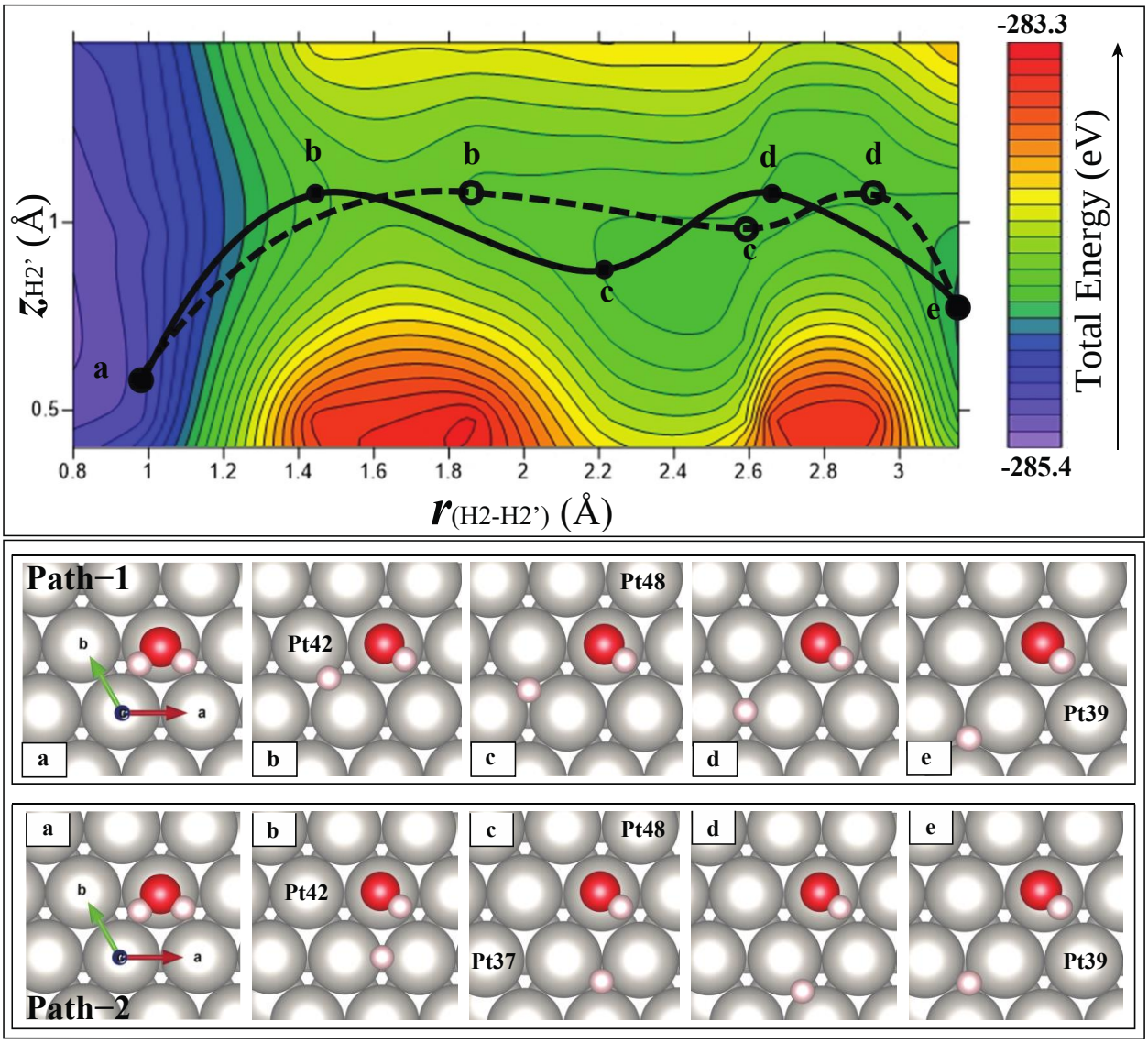

Figure 2: (upper) Two dimensions contour profile of potential energy surfaces (PESs) for Path-1 (solid line) and Path-2 (dashes line) as a function of r, z. The H2' distance from the surface is z-H2' and H2'−OH1 is the distance of H2' variation from OH1. (lower) The reaction coordinates for H_2O dissociation for two pathways.

Figure 2 shows the PESs results for Path-1 and Path-2 with the points of *a* to the *e* point in the PES plot corresponds to the configuration for each path as the H2' position separated away from OH1. In the reaction pathway number-1 (Path-1), H2' start to moves from its original position (H2) to bridge site of (Pt42 and Pt38), then proceed to the hollow hcp site to bridge (Pt37 and Pt38) site and the final position is at hollow fcc site as shown in figure 2 below the 2D countour plot. As the Path-2, the reaction coordinates proceed with order bridge site (of Pt42−Pt38) to hollow fcc to bridge site (of Pt34−Pt38) and endup in hollow fcc sites as shown in figure 2 Path-2. From the total energy at the side levels in the figure 2, the transition state (TS) occur at point *b* for the two reaction pathways (Path-1 and Path-2) when the H2' position at bridge site of Pt42−Pt38 and Pt38−Pt39, respectively. Based on the corresponding PESs scan from figure 2, we obtained that TS-2 is

higher than TS-1 with respect to IS with the energy barrier of 0.80 eV and 0.83 eV, respectively, presented in figure 3(a). Thus the path-1 is preferable pathway as the activation energy lower than path-2. Therefore, between the two pathways of our investigations from the PESs scan, we then conclude that the prefered path between the two, the path-1 is the most possible pathway in the dissociation of H_2O into OH_{ads} and H_{ads} on Pt(111) surface. The two coordinate reaction pathways are summarized in figure 3(a)(b) with its corresponding activation energies. The energy difference between the two paths from our calculation results showed not so significantly different i.e., 0.03 eV. Our calculated energy barriers are agree well to the other DFT calculation by Fajin et al. (0.78 eV) [37] and Phatak et al. (0.75 eV) [20]. This suggest that our proposed reaction cooordinates becomes possible in dissociating H_2O_{ads}/Pt(111) into (OH_{ads}+H_{ads})/Pt(111).

Table I: The charge density profile at IS, TSs, and FS along the most minimum energy path of H_2O dissociation on Pt(111). Positive and negative signs indicates the atom excess and deficit electrons respectively.

No.	State	H2' adsorbed positions	$r_{e(OH1\text{-}H2')}$ [Å]	$z\text{-}_{(H2')}$ [Å]	Charge gain or loss [e−]	
1.	IS	H2'@[H_2O/Pt−43]	0.98	2.31	[O]=−0.47; [H1]=+0.48; [H2']=+0.45	[Pt43]=−0.23
2.	TS Path-1	H2'@[Pt38−Pt42]	1.44	1.07	[O]=+0.09; [H1]=+0.50; [H2']=+0.91	[Pt42]=−0.39 [Pt38]=−0.45
3.	TS Path-2	H2'@[Pt38−Pt39]	1.86	1.07	[O]=+0.12; [H1]=+0.45; [H2']=+1.01	[Pt38]=−0.43 [Pt39]=−0.42
4.	FS	H2'@[Pt33−Pt37−Pt38]	3.15	0.77	[O]=+0.14; [H1]=+0.43; [H2']=+0.86	[Pt33]=−0.13 [Pt37]=−0.15 [Pt38]=−0.59

Finally, the projected density of states (PDOS) profile and charge density difference for Pt related atoms and atomic O, H1 and H2' over Pt(111) at IS, TS and FS will be expanded in figure 3(c) − 3(f) and table I. The corresponding atomic projected DOS of TS for Path-1 and Path-2 of five atoms are presented in figure 3(c) and 3(d) respectively, which describes the local DOS of figure 3(b) for two TSs. One must note that an additional localized state become apparent at low energy level, which leads to the resonance state of the adsorbed oxygen−hydrogen and related Pt atom. The involvement of the electrons of Pt atom far below the Fermi level of the metal plays important role for these states as the resonance states mainly consist of (*s*) and (*d*) states of Pt atom and (*s*) and (*p*) from hydrogen and oxygen. The broadening states of hybridization between atomic Pt and H2' states at Path-1 is larger than the case at Path-2, which leads the resonance peak of PDOS on Path-1 is lower than on Path-2. This corroborate with the result that the TS energy of Path-1 is lower than that of TS energy of Path-2 during the reaction pathways.

Table I shows the adsorbed structure of H2' while OH1 being fixed at Pt43 site, the distance *r*-(OH1−H2), *z*-H2′ , and the charge density difference profile of atom O, H1, H2' as well as the related Pt atom at IS, TS and FS. The adsorbed H_2O molecule on Pt43 as the initial state has minimal atomic charge density with negative value of atomic O, that might caused by the bonding formation of H_2O adsorbed at Pt(111) surface. This also supported by the elongated H_2O bond distance at adsorbed state on Pt(111) by ~0.01 Å with reference to the gas phase. The weakening of O−H2 bond might leads to bond breaking into other possible species i.e., OH_{ads} and H_{ads} or O_{ads} and two H_{ads}. In this case, we only focus on the separation of H_2O into OH_{ads} and H_{ads} as our concern. As we move H2' separated away from OH1 bond, along the reaction pathways, the TS-1 and TS-2 has the maximum charge depositions with gaining the positive charge of O and H2' atoms.

The H2' gains more electrons presumably comes from the surface as the H2' makes a new bond with Pt surfaces after dissociate from OH1 bond. At the FS, H2' has reached the longest distance from OH1 bond that ensure the dissociation species is far enough at 3.15 Å. The atomic O becomes more electronegative because the excess in electrons as compared in TSs. In this state, the H2' has also gain the electrons but less than that in TSs in which makes H2' becomes more stable in the form of absorbed H. Between the two pathways, the increasing charge transfer from Pt surface to the adsorbates may lead to reducing the energy barrier as predicted by Cahyanto, et al., [36] and this also consistent with our predicted results (i.e., TS-1 < TS-2). The final results of our configuration in dissociating H_2O molecule into OH_{ads} and H_{ads} fractions might becomes possible pathways that could explain the dissociation mechanism of monomeric H_2O on Pt(111) surface.

4. SUMMARY AND CONCLUSION

In summary, we have proposed two possible reaction pathways of H_2O dissociation into OH_{ads} and

H_{ads} over the Pt(111) by PESs based on density functional theory calculations. We considered the path as the possible shortest distance from initial state to final state configuration. Our results show the two proposed pathways (Path-1 and Path-2) are almost similar value of of 0.80 and 0.83 eV respectively. This results is very close to the other DFT calculation results in which suggest that our two reaction coordinates are possible pathway in decomposing H_2O_{ads} into (OH_{ads}+H_{ads})/Pt(111) surface. Yet, calculations results presented here should be able to give the insight in developing catalyst for water dissociation in contribution of the reaction rate in H_2O dissociation on Pt-based catalyst.

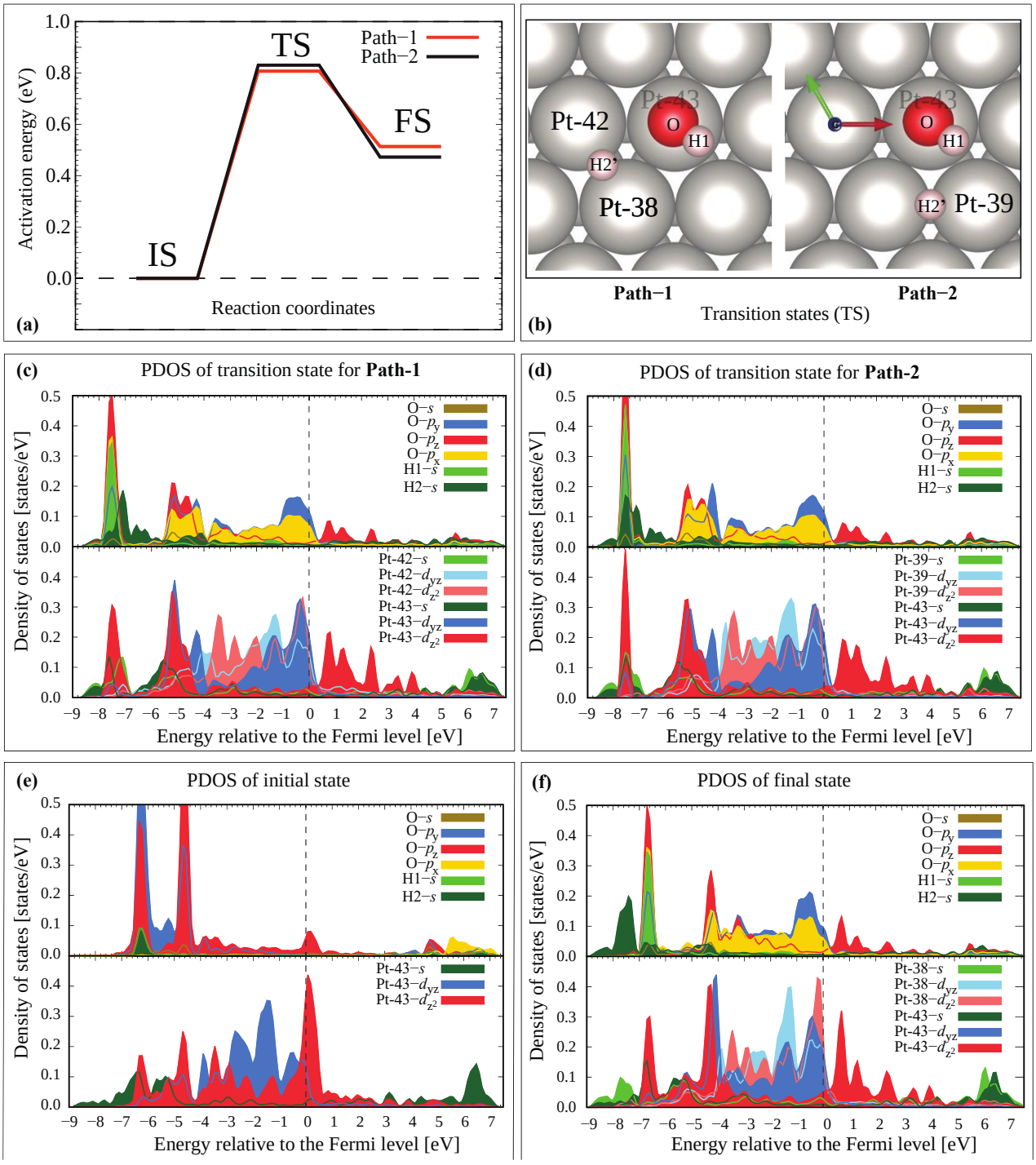

Figure 3: (a) The calculated results of energy barrier along the reaction coordinates for each path with respect to the IS configuration. (b) Transition states configurations of Path-1 and Path-2. (c) Atomic projected DOS during the interaction of Path-1. (d) Atomic projected DOS during the interaction of Path-2. (e) and (f) are atomic projected DOS during the IS and FS respectively.

AUTHORS' CONTRIBUTIONS

W.T.C. designed and arranged the project; S.Z. developed the model system, conducted the calculations, analysed the data, and wrote the manuscript; A.A.B.P discussed the electronic structures; D.N.W.D conduct the rest of calculation and discussed the results.

ACKNOWLEDGMENTS

All calculations were performed using computer series at Laboratorium Fisika Komputasi Material UNSOED.

REFERENCES

[1] A. Olabi, T. Wilberforce, and M. A. Abdelkareem, Energy 214, 118955 (2021). DOI: https://doi.org/10.1016/j.energy.2020.118955
[2] J. D. Holladay, J. Hu, D. L. King, and Y. Wang, Catalysis today 139, 244 (2009). DOI: https://doi.org/10.1016/j.cattod.2008.08.039
[3] D. Pal, R. Chand, S. Upadhyay, and P. Mishra, Renewable and Sustainable Energy Reviews 93, 549 (2018). DOI: https://doi.org/10.1016/j.rser.2018.05.003
[4] D. S. Newsome, Catalysis Reviews Science and Engineering 21, 275 (1980). DOI: https://doi.org/10.1080/03602458008067535
[5] D. Grenoble, M. Estadt, and D. Ollis, Journal of Catalysis 67, 90 (1981). DOI: https://doi.org/10.1016/0021-9517(81)90263-3
[6] H. R. Colón-Mercado and D. T. Hobbs, Electrochemistry communications 9, 2649 (2007). DOI: https://doi.org/10.1016/j.elecom.2007.08.015
[7] A. Appleby and B. Pinchon, International Journal of Hydrogen Energy 5, 253 (1980). DOI: https://doi.org/10.1016/0360-3199(80)90070-1
[8] P. Lu and R. Ammon, Journal of the Electrochemical Society 127, 2610 (1980). DOI: https://doi.org/10.1149/1.2129530
[9] P. A. Thiel and T. E. Madey, Surface Science Reports 7, 211 (1987). DOI: https://doi.org/10.1016/0167-5729(87)90001-X
[10] M. A. Henderson, Surface Science Reports 46, 1 (2002). DOI: https://doi.org/10.1016/S0167-5729(01)00020-6
[11] M. Morgenstern, T. Michely, and G. Comsa, Physical review letters 77, 703 (1996). DOI: https://doi.org/10.1103/PhysRevLett.77.703
[12] K. Motobayashi, L. Árnadóttir, C. Matsumoto, E. M. Stuve, H. Jónsson, Y. Kim, and M. Kawai, ACS nano 8, 11583 (2014). DOI: https://doi.org/10.1021/nn504824z
[13] A. Glebov, A. Graham, and A. Menzel, Surface science 427, 22 (1999). DOI: https://doi.org/10.1016/S0039-6028(99)00228-9
[14] Q.-L. Tang and Z.-P. Liu, The Journal of Physical Chemistry C 114, 8423 (2010). DOI: https://doi.org/10.1021/jp100864j
[15] A. A. Gokhale, J. A. Dumesic, and M. Mavrikakis, Journal of the American Chemical Society 130, 1402 (2008). DOI: https://doi.org/10.1021/ja0768237
[16] J. L. Fajín, M. N. D. Cordeiro, F. Illas, and J. R. Gomes, Journal of Catalysis 268, 131 (2009). DOI: https://doi.org/10.1016/j.jcat.2009.09.011
[17] E. Ticanelli, J. Beery, M. Paffett, and S. Gottesfeld, Journal of electroanalytical chemistry and interfacial elec- trochemistry 258, 61 (1989). DOI: https://doi.org/10.1016/0022-0728(89)85162-9
[18] H. A. Gasteiger, N. Markovic´, P. N. Ross Jr, and E. J. Cairns, Electrochimica Acta 39, 1825 (1994). DOI: https://doi.org/10.1016/0013-4686(94)85171-9
[19] S. Seong and A. B. Anderson, The Journal of Physical Chemistry 100, 11744 (1996). DOI: https://doi.org/10.1021/jp9610877
[20] A. A. Phatak, W. N. Delgass, F. H. Ribeiro, and W. F. Schneider, The Journal of Physical chemistry c 113, 7269 (2009). DOI: https://doi.org/10.1021/jp810216b
[21] E. M. Karp, C. T. Campbell, F. Studt, F. Abild-Pedersen, and J. K. Nørskov, The Journal of Physical Chemistry C 116, 25772 (2012). DOI: https://doi.org/10.1021/jp3066794
[22] P. Hohenberg and W. Kohn, Phys. Rev. 136, B864 (1964). DOI: https://doi.org/10.1103/PhysRev.136.B864
[23] W. Kohn and L. J. Sham, Phys. Rev. 140, A1133 (1965). DOI: https://doi.org/10.1103/PhysRev.140.A1133
[24] G. Kresse and J. Hafner, Physical review B 47, 558 (1993). DOI: https://doi.org/10.1103/PhysRevB.47.558
[25] G. Kresse and J. Furthmüller, Computational materials science 6, 15 (1996). DOI: https://doi.org/10.1016/0927-0256(96)00008-0
[26] P. E. Blöchl, Physical review B 50, 17953 (1994). DOI: https://doi.org/10.1103/PhysRevB.50.17953
[27] G. Kresse and D. Joubert, Physical review b 59, 1758 (1999). DOI: https://doi.org/10.1103/PhysRevB.59.1758
[28] J. P. Perdew, J. Chevary, S. Vosko, K. A. Jackson, M. R. Pederson, D. Singh, and C. Fiolhais, Physical Review B 48, 4978 (1993). https://doi.org/10.1103/PhysRevB.48.4978.2
[29] J. P. Perdew, K. Burke, and M. Ernzerhof, Physical review letters 77, 3865 (1996). DOI: https://doi.org/10.1103/PhysRevLett.77.3865
[30] J. White and D. Bird, Physical Review B 50, 4954 (1994). DOI: https://doi.org/10.1103/PhysRevB.50.4954
[31] H. J. Monkhorst and J. D. Pack, Physical review B 13, 5188 (1976). DOI: https://doi.org/10.1103/PhysRevB.13.5188
[32] M. Methfessel and A. Paxton, Physical Review B 40, 3616 (1989). DOI: https://doi.org/10.1103/PhysRevB.40.3616
[33] S. Zulaehah, W. Cahyanto, I. Fitriani, F. Abdullatif, W. Widanarto, and M. Effendi, in Journal of Physics: Conference Series, Vol. 1494 (IOP Publishing, 2020)

p. 012040. DOI: https://doi.org/10.1088/1742-6596/1494/1/012040
[34] V. Branger, V. Pelosin, K. Badawi, and P. Goudeau, Thin Solid Films 275, 22 (1996). DOI: https://doi.org/10.1016/0040-6090(95)07011-7
[35] W. T. Cahyanto, S. Zulaehah, F. Abdullatif, W. Widanarto, M. Effendi, and H. Kasai, Journal of Electronic Materials 49, 2642 (2020). DOI: https://doi.org/10.1007/s11664-020-07976-4
[36] W. T. Cahyanto, S. Zulaehah, W. Widanarto, F. Abdullatif, M. Effendi, and H. Kasai, ACS omega 6, 10770 (2021). DOI: https://doi.org/10.1021/acsomega.1c00389
[37] J. L. Fajín, M. N. DS Cordeiro, and J. R. Gomes, The Journal of Physical Chemistry A 118, 5832 (2014). DOI: https://doi.org/10.1021/jp411500j
[38] B. Hammer and J. K. Nørskov, Advances in catalysis 45, 71 (2000). DOI: https://doi.org/10.1016/S0360-0564(02)45013-4